Металлофиз. новейшие технол. / Metallofiz. Noveishie Tekhnol.
2013, т. 35, № 2, сс. 209–223
Оттиски доступны непосредственно от издателя
Фотокопирование разрешено только
в соответствии с лицензией

PACS numbers: 61.72.Hh, 62.20.Qp, 62.25.-g, 62.40.+i, 64.60.Cn, 81.30.Hd, 81.70.Pg

Study of Ordering in Fe–25% Al–Cr Alloys by Dilatometry, Heat Flow and Mechanical Spectroscopy

Z. Belamri, D. Hamana, I. S. Golovin*, and I. B. Chudakov**

Research Unit on Materials Science and Applications,
Mentouri University of Constantine,
Ain El Bey Road, 325,
25000 Constantine, Algeria
**National Research Technological University 'MISiS',*
Leninskiy Ave., 4,
119049 Moscow, Russia
***State Research Center of Russian Federation*
'I. P. Bardin Central Research Institute for Ferrous Metallurgy',
2nd Baumanskaya Str., 9/23,
105005 Moscow, Russia

It is known that the addition of Cr to the Fe_3Al-based alloys leads to an improvement in their ductility and other properties. In a given work, dilatometric, differential scanning calorimetric (DSC) and internal friction tests are performed to study the ordering process in stoichiometric and overstoichiometric Fe_3Al alloys with Cr addition at a constant heating rate from room temperature up to 1000°C. The results indicate that the addition of Cr slows the $D0_3$-type ordering process; this can be confirmed by obtained values of activation energy. Cr addition has also an effect on the mechanical properties of studied alloys annealed in $D0_3$-type order domain. The heights and broadening of three peaks (of X-, Zener-, and Snoek-type) can be changed at the presence of Cr. X-ray diffraction (XRD) and TEM studies are carried out at different temperatures chosen from the obtained DSC curves and affirmed that a rapid quenching just after heat treatment from highest temperature cannot suppress the formation of $B2$ ordered particles in overstoichiometric Fe_3Al alloys.

Відомо, що додавання Cr до стопів на основі Fe_3Al спричиняє поліпшення їх пластичности та інших властивостей. У даній статті виконано дилатометричні випробування та випробування методами диференційної скануючої калориметрії (ДСК) і внутрішнього тертя з метою вивчення процесу впорядкування в стехіометричних та надстехіометричних стопах Fe_3Al з додаванням Cr при сталій швидкості нагрівання від кімнатної температури до 1000°C. Додавання Cr сповільнює процес упорядкування за над-

структурним типом $D0_3$, що підтверджується одержаними значеннями енергії активації. Додавання хрому впливає також на механічні властивості досліджених стопів, відпалених в області $D0_3$-порядку. Висоти та розширення трьох піків (Зінерового, Снукового та Х-типу) можуть змінюватися в присутності Cr. Рентґенодифракційна аналіза та трансмісійна електронна мікроскопія, виконані за різних температур, обраних на підставі одержаних ДСК-кривих, підтвердили, що швидке гартування від самої високої температури зразу після теплового оброблення не може пригнітити формування впорядкованих частинок типу $B2$ у надстехіометричних стопах Fe_3Al.

Известно, что добавление Cr к сплавам на основе Fe_3Al приводит к улучшению их пластичности и других свойств. В данной статье выполнены дилатометрические испытания и испытания методами дифференциальной сканирующей калориметрии (ДСК) и внутреннего трения с целью изучения процесса упорядочения в стехиометрических и сверхстехиометрических сплавах Fe_3Al с добавлением Cr при постоянной скорости нагрева от комнатной температуры до 1000°C. Добавление Cr замедляет процесс упорядочения по сверхструктурному типу $D0_3$, что подтверждается полученными значениями энергии активации. Добавление хрома влияет также на механические свойства исследуемых сплавов, отжигаемых в области $D0_3$-порядка. Высоты и уширение трёх пиков (зинеровского, снуковского и Х-типа) могут изменяться в присутствии Cr. Рентгенодифракционный анализ и просвечивающая электронная микроскопия, выполненные при различных температурах, выбранных на основании полученных ДСК-кривых, подтвердили, что быстрая закалка от самой высокой температуры сразу после тепловой обработки не может подавить формирование упорядоченных частиц типа $B2$ в сверхстехиометрических сплавах Fe_3Al.

Key words: intermetallics, ordering, phase transformation, dilatometry, hardness measurement, internal friction.

(Received September 11, 2012)

1. INTRODUCTION

Properties of the Fe–Al alloys are low density, high melting temperature and hardness, a good oxidation resistance coupled with a good resistance to the fracture. They create a large prospect for the Fe–Al alloys industrial application, for example as components of the machines used at high temperature, in corrosive environment (Refs. 6–9 cited by [1–3]) or as high damping alloys [4–6]. However, these materials have a low ductility at room and elevated temperature [7]. The ductility and corrosion resistance can be improved by the addition of a third element, for example chromium. The field of application of ternary Fe–Al–Cr alloys is very vast, primarily as substrate for a catalyst applied in the catalytic converters and as filter in automobiles [8].

An important feature of this system is the high solubility of both Al

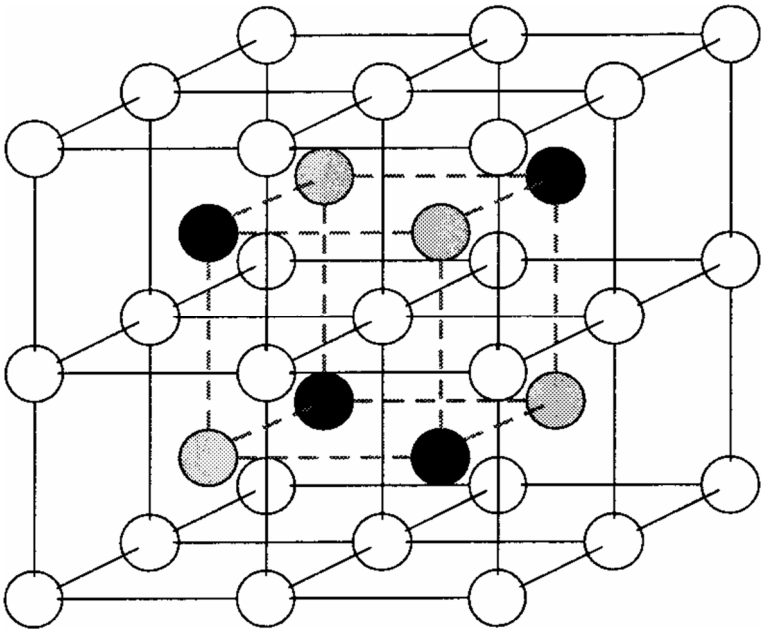

Fig. 1. Lattice structure in Fe_3Al: 4a (Al) positions—full circles, 4b (Fe)—grey circles, and 8c (Fe)—open circles.

and Cr in b.c.c. iron. The Cr atoms occupy most probably the 4b or 8c positions (Fig. 1) with some preference of next nearest neighbour Al positions [9]. The dissociation energy for Cr–Al pairs ($W_{(Cr-Al)}$ = = 0.6960 eV) that is lower than for Fe–Al pairs ($W_{(Fe-Al)} = 0.7457$ eV) is responsible for the mentioned decrease of the antiphase boundary (APB) energy. The density of vacancies in Fe–25Al–(15–25)Cr alloys quenched from 1273 K was detected to be about $c_V \approx 3 \cdot 10^{-5}$ at^{-1}, which is three times lower than that in Fe–25Al ($c_V \approx 10^{-4}$ at^{-1} [10]) but higher than it is in Fe–Si–Al alloys.

Recent studies show the utility of the addition of Cr in Fe–Al based alloys; the Fe–(25–28)Al* alloys are often alloyed with 3–5% Cr to increase their ductility and their workability (Ref. 1 cited by [11]). Sikka *et al.* [12] observed that ductility at room temperature in Fe–28Al alloy was increased by the addition of 5% Cr. McKamey *et al.* [13] show that the addition of 6% Cr leads to the increase in ductility at low temperature from 4% to 8–10% approximately. Since the dissociation energy $W_{(Cr-Al)}$ is lower than $W_{(Fe-Al)}$, it results in an improvement of the intrinsic ductility of Fe_3Al due to the decrease in the energy of the antiphase boundary, increasing the mobility and the slip of dislocations

*All compositions in this paper are given in atomic percents.

(Ref. 28 cited by [11] and [14]). The presence of Cr in Fe–28Al–3Cr alloy improves the pitting corrosion resistance by the increase of the pitting potential of the alloy [15].

Chromium does not have a significant effect on the value of the transition temperature from $D0_3$ to $B2$ (T_0) phases and slightly increases the transition interval $A2 \rightarrow D0_3$ of quenched $(Fe,Cr)_3Al$ alloys according to the differential scanning calorimetric (DSC) data showed in this work. Hamana *et al.* [16] showed that the ternary element (addition of 2% Cr and 5% Cr in Fe–28Al alloy) stabilizes the $B2$ ordered phase and slows the $B2 \rightarrow D0_3$ transition.

The purpose of this paper is to study the order–disorder transition in Fe–Al–Cr alloys using differential scanning calorimetry, dilatometry, and related internal friction effects by mechanical spectroscopy technique.

2. MATERIALS AND EXPERIMENTAL METHODS

The alloys used in this work have the following compositions: Fe–25Al–25Cr, Fe–25Al–9Cr, Fe–28Al–4Cr and Fe–27Al–2Cr. Before characterization, the samples were homogenized for one hour at 1000°C and water quenched. The samples have a cylindrical shape for the dilatometric analysis (12×3 mm), and for the DSC analysis (5×5 mm).

For tests a DSC 131 SETARAM and DI24 ADAMEL LHOMARGY dilatometer connected to a computer respectively were used; suitable software allows analysing and determining the critical points on the recorded curves. The internal friction (IF), *i.e.* damping Q^{-1}, is measured as a function of temperature at vibrating reed setup at resonance frequency of one side clamped sample with $\varepsilon_0 \approx 10^{-5}$.

The microhardness is measured with a load of 3 N using a ZWICK apparatus connected to the computer with adapted software provided the values of HV automatically.

To identify the type of phases appearing in the studied alloys, Siemens D8 Advance diffractometer is used. The recorded XRD patterns were obtained with Cu anticathode (I = 40 mA, V = 40 kV). The transmission electron microscopy (Philips CM12) is used for the characterization of the alloys.

3. RESULTS AND DISCUSSIONS

Specimens were characterized at heating and cooling by DSC, dilatometry and internal friction measurements. X-ray diffraction (XRD) and TEM studies were performed after chosen heat treatment regimes.

3.1. Differential Scanning Calorimetric Study

The DSC curves obtained with heating rate of 10°C/min (Figs. 2, *a*–*d*) of

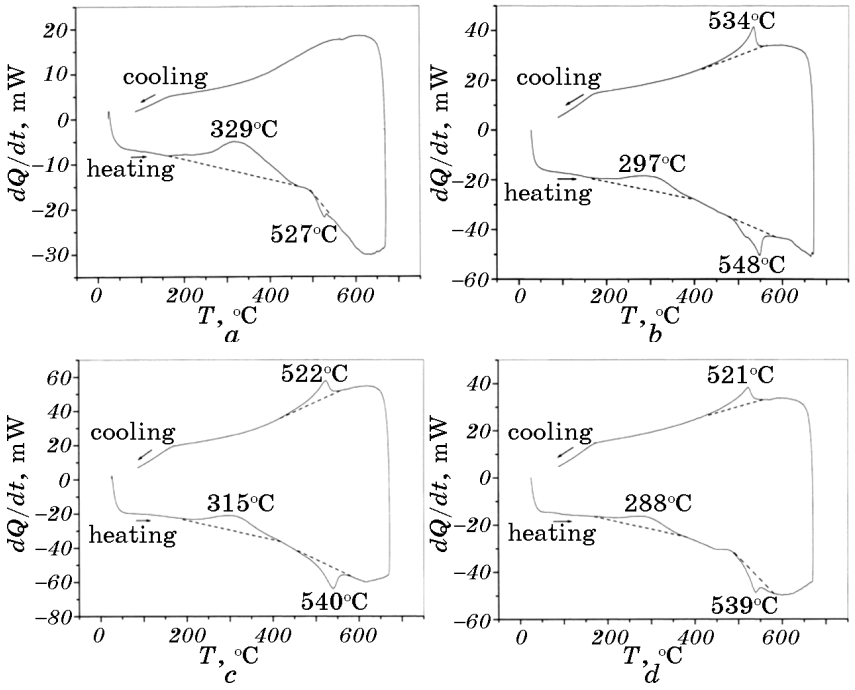

Fig. 2. DSC curves of the homogenised 1 h at 1000°C and water quenched (heating rate = 10°C/min): Fe–25Al–25Cr (*a*), Fe–25Al–9Cr (*b*), Fe–28Al–4Cr (*c*), Fe–27Al–2Cr (*d*) alloys.

homogenised 1 h at 1000°C and water quenched Fe–25Al–25Cr, Fe–25Al–9Cr, Fe–28Al–4Cr, Fe–27Al–2Cr alloys, respectively, demonstrate the following effects.

An exothermic peak linked to the formation of the ordered phase from α partial disordered state. Nevertheless, we can detect some order by XRD after water quenching of these alloys (see below in Figs. 5, *a*–*d*). TEM micrograph of water quenched Fe–26Al sample [17] shows antiphase boundaries with large $B2$ domain and very fine $D0_3$ domains can be distinguished. According to Allen (Ref. 9 cited by [18]), this transition undergoes the following sequence: $\alpha \rightarrow B2 \rightarrow$ $\rightarrow D0_3$ in overstoichiometric Fe–Al alloys. $B2$ order is also found in Fe–25Al–25Cr after quenching from 1250 K (Fig. 3, *a*). Therefore, the rapid quenching of studied alloys after heat treatment at high temperature cannot suppress the formation of the $B2$ ordered particles. $D0_3$ domains were observed by TEM in Fe–25Al–9Cr, while $B2$ and $D0_3$ domains are observed in Fe–25Al–25Cr composition after annealing at 748 K and quenching. In TEM micrographs of these two alloys (see Figs. 3, *b*, *c*), fine $D0_3$ domains for Fe–25Al–25Cr (domains are fine because the temperature is rather close to the $D0_3$ to

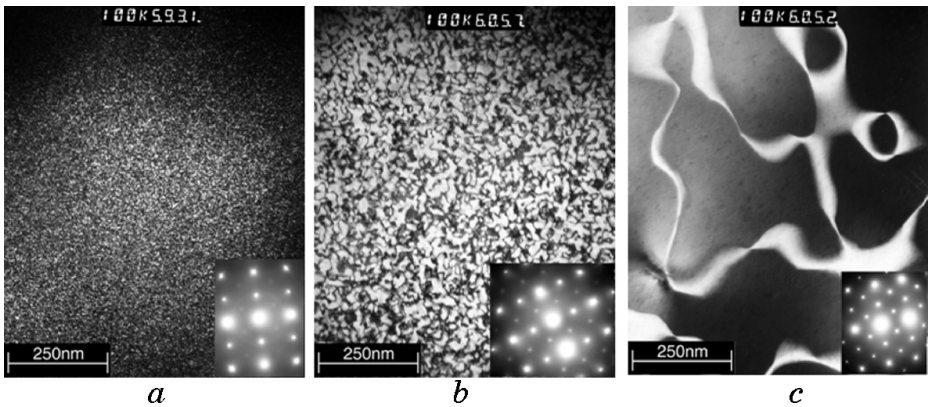

Fig. 3. TEM micrographs of Fe–25Al–25Cr alloy homogenized at 1000°C and water quenched (*a*), Fe–25Al–25Cr sample water quenched from 1000°C then annealing 48 h at 475°C (*b*), Fe–25Al–9Cr sample water quenched from 1000°C then annealing 48 h at 475°C (*c*).

$B2$ transition) and coarse $D0_3$ domains for Fe–25Al–9Cr are presented. Cooling rate of the Fe–25Al–25Cr alloy has a great influence on the type of order: $B2$ or $D0_3$ [19].

An endothermic peak caused by the decrease in the order of the $D0_3$ ordered phase and the formation of the $B2$ ordered phase.

An exothermic peak is observed during cooling, which corresponds to the $B2 \rightarrow D0_3$ transition on all DSC curves; however, on the DSC curve of Fe–25Al–25Cr this peak is broad and it is difficult to specify temperature: high amount of Cr slows the transition.

It should be noted that the effects observed on the DSC curves in studied Fe–Al–Cr alloys are rather similar to those in binary Fe–Al alloys [18]. The influence of composition of studied alloys on order–disorder transition temperatures is summarized in Table 1.

TABLE 1. Nominal composition, phase transitions temperatures of studied alloys according to the DSC and dilatometric analysis (heating/cooling rate 10°C/min).

Nominal composition	DSC (heating + cooling)			Dilatometry (heating)	
	$\alpha + D0_3 \rightarrow D0_3$	$D0_3 \rightarrow B2$	$B2 \rightarrow D0_3$	$\alpha + D0_3 \rightarrow D0_3$	$D0_3 \rightarrow B2$
Fe–25Al–25Cr	329°C	527°C	*	327°C	546°C
Fe–25Al–9Cr	297°C	548°C	534°C	255°C	550°C
Fe–28Al–4Cr	315°C	540°C	522°C	260°C	542°C
Fe–27Al–2Cr	288°C	539°C	521°C	247°C	538°C

* It is impossible to specify temperature.

3.2. Dilatometric Study

Dilatometric curves of the homogenised 1 h at 1000°C and water quenched Fe–25Al–25Cr, Fe–25Al–9Cr, Fe–28Al–4Cr and Fe–27Al–2Cr samples, obtained with a heating rate of 10°C/min (Figs. 4, *a–d*) respectively, show an important anomaly and the derivative heating curves show the following effects: contraction caused by the formation of the $D0_3$ ordered phase starting from the α disordered phase; expansion caused by the decrease in the order of $D0_3$ ordered phase and the formation of the $B2$ ordered phase.

In general, the dilatometry data confirm the heat flow data. Some insignificant quantitative differences are caused by different sensitivity of these methods.

3.3. XRD Study

XRD analysis is carried out in order to confirm the nature of the phases responsible for the appearance of the effects at DSC and dilatometric curves during heating. All samples were homogenised 1 h at 1000°C, and then heated up to the maximum temperatures of DSC peaks and water quenched. The XRD patterns of the homogenized and water

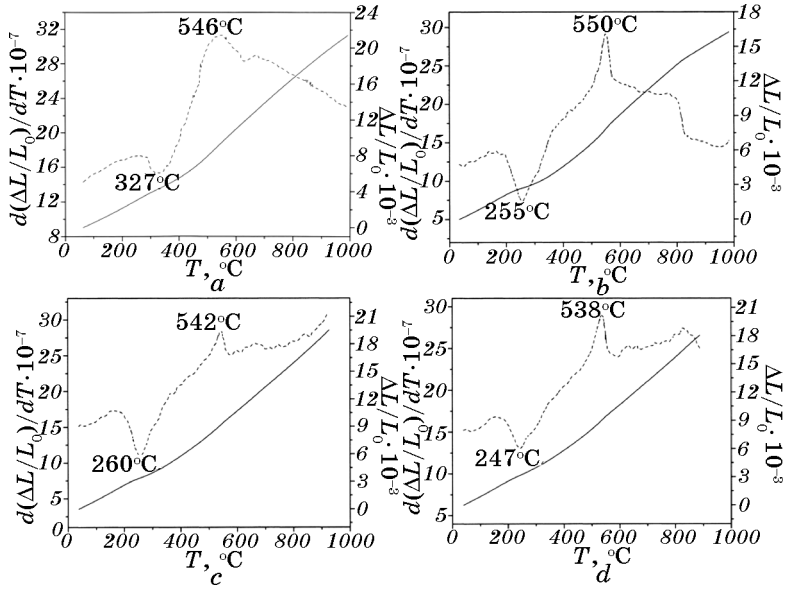

Fig. 4. Dilatometric heating curves of the homogenised 1 h at 1000°C and water quenched (heating rate = 10°C/min): Fe–25Al–25Cr (*a*), Fe–25Al–9Cr (*b*), Fe–28Al–4Cr (*c*), Fe–27Al–2Cr (*d*) alloys; solid line—derivative heating curve, dotted line—heating.

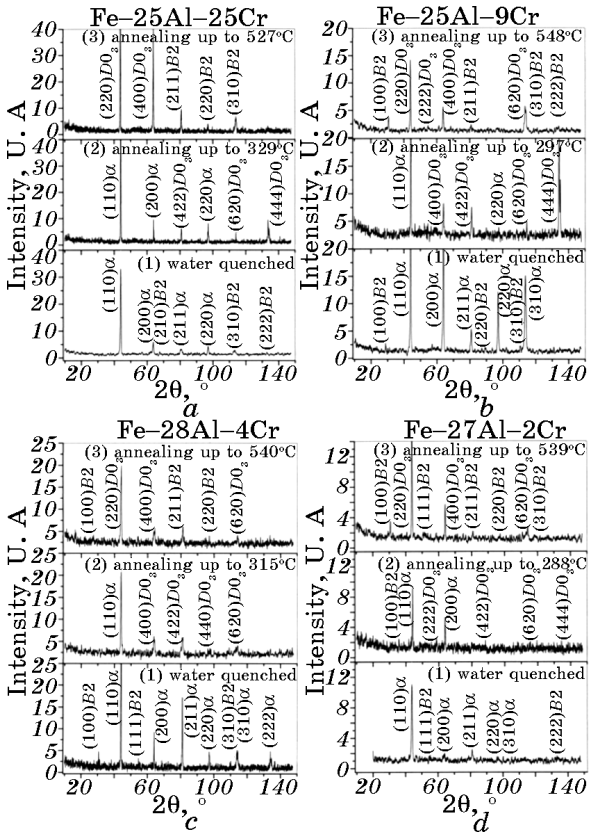

Fig. 5. XRD patterns of Fe–25Al–Cr alloys after homogenised 1 h at 1000°C and water quenched then heating up to deferent temperatures indicated on each figure.

quenched alloys show the peaks of α disordered phase with small peaks corresponding to the *B*2 ordered phase (Figs. 5, *a*–*d*). Table 2 summarises the obtained results of XRD analysis of each alloy.

3.4. Determination of the Activation Energy of Ordering

Starink (Eq. (1), [20]), Kissinger (Eq. (2), [21]), and Ozawa (Eq. (3), [22]) methods are used to estimate activation energy of the $D0_3$ ordering process in the studied alloys. The heat flow (DSC) measurements are carried out at four different heating rates: 10, 15, 20 and 25°C/min. The variations of the temperature of the maximum of the first exothermic peaks (T_m) with a heating rate β:

$$\ln(\beta / T_m^{1.92}) = -1.0008(E_{act} / RT_m) + C_1 , \quad (1)$$

TABLE 2. The different phases obtained by XRD in studied alloys after heat treatments.

Alloy	Water quenched after heating up to	Structure of phases
Fe–25Al–25Cr	329°C	$A2 + D0_3$
	527°C	$D0_3 + B2$
Fe–25Al–9Cr	297°C	$A2 + D0_3$
	548°C	$D0_3 + B2$
Fe–28Al–4Cr	315°C	$A2 + D0_3$
	540°C	$D0_3 + B2$
Fe–27Al–2Cr	288°C	$A2 + D0_3$
	539°C	$D0_3 + B2$

$$\ln(\beta / T_m^2) = -E_{act} / RT_m + C_2 , \quad (2)$$

$$\ln \beta = -1.0516(E_{act} / RT_m) + C_3 . \quad (3)$$

Figures 6, *a*–*d* show the superposition of DSC curves of studied alloys, where the exothermic peak related to the formation of $D0_3$ ordered phase appears; they reveal that the increase of the heating rate β leads to the shift of the maximum of the exothermic peaks toward high temperatures.

The activation energy of ordering process of the $D0_3$ phase (Table 3) in the studied alloys is deduced from the different methods presented in Figs. 7, *a*–*d*. All three methods give almost the same values for each alloy.

The value of the activation energy rises with the increase of the Cr content in Fe_3Al compound, which means that the ordering process of $D0_3$ ordered phase formation in the alloy with higher Cr amount requires more energy. The diffusion coefficient is governed by the exponential law [23]:

$$D = D_0 \exp(-E_{act} / RT) . \quad (4)$$

If the value of the E_{act} is high, the diffusion is slow; thus, the addition of chromium slows the ordering process. It is in agreement with the results obtained by the dilatometric and differential calorimetric analysis.

3.5. Temperature Dependent Internal Friction

Internal friction spectra of binary Fe–Al alloys have been studied by several researchers [24]: at least three thermally activated peaks were recorded at elevated temperatures: the carbon Snoek (S), Zener (Z) re-

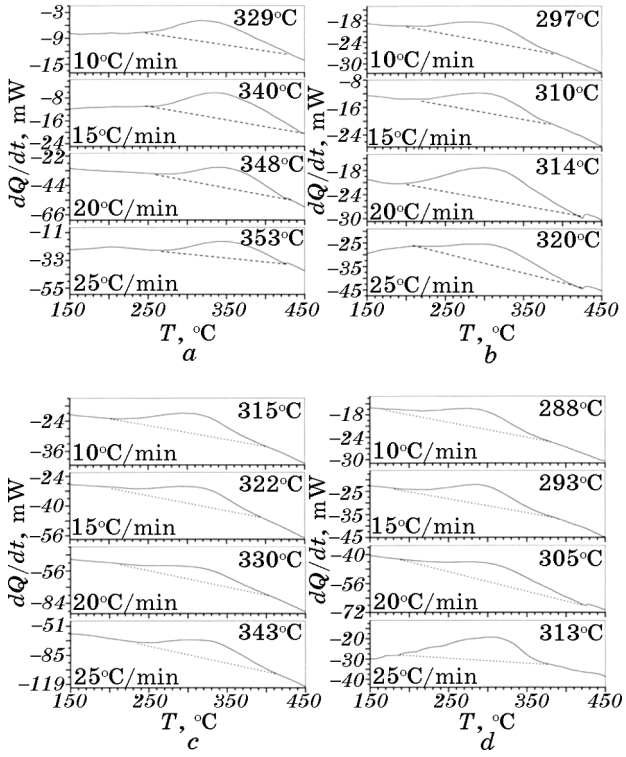

Fig. 6. Parts of DSC curves corresponding to the $D0_3$ ordered phase formation in homogenised 1 h at 1000°C, water quenched then heated with various rates Fe–25Al–25Cr (*a*), Fe–25Al–9Cr (*b*), Fe–28Al–4Cr (*c*), Fe–27Al–2Cr (*d*) alloys.

laxations and less explained (X) effect; they are caused by the presence of structural vacancies and carbon atoms in alloys. Chromium is a carbide-forming element both in iron and in Fe–Al-based alloys. Calculations [25] have demonstrated that the C–Cr 'chemical' plus 'elastic' interatomic interaction in iron takes place up to the fifth coordination shell, however, some interstitial carbon remains in solid solution after water quenching [26]; that results in the appearance of the so-called Snoek-type peak [10] (denoted as the S peak in Fig. 8).

If the Al content exceeds the Cr content, the Snoek-type peak shifts to higher temperatures than those of Fe–31Al, which is caused by the additional C–Cr interaction [27], while the Snoek-type peak height decrease is caused by the decrease in the carbon amount in solid solution. The X peak also recorded in Fig. 8 was interpreted earlier [28, 29] as a relaxation peak caused by C-vacancy reorientation in the applied stress field. For the case of a fixed Al content (≅ 25 at.%) and Cr substituting Fe, all above-mentioned tendencies can also be seen but the relative

TABLE 3. Activation energy values of ordering process of the $D0_3$ ordered phase formed during heating in homogenised 1 hour at 1000°C and water quenched samples, estimated by three methods.

Alloy	Activation energy E_{act}, eV		
	Methods		
	Starink's	Kissinger's	Ozawa's
Fe–25Al–25Cr	1.31 ± 0.19	1.31 ± 0.19	1.34 ± 0.18
Fe–25Al–9Cr	1.25 ± 0.23	1.25 ± 0.23	1.28 ± 0.22
Fe–28Al–4Cr	1.10 ± 0.11	1.09 ± 0.11	1.14 ± 0.11
Fe–27Al–2Cr	1.04 ± 0.17	1.04 ± 0.17	1.08 ± 0.16

changes are different (see Fig. 8).

The high Cr addition has a remarkable effect on the damping capacity of Fe_3Al based alloys. Below 450°C (Fig. 8), progressive decrease of

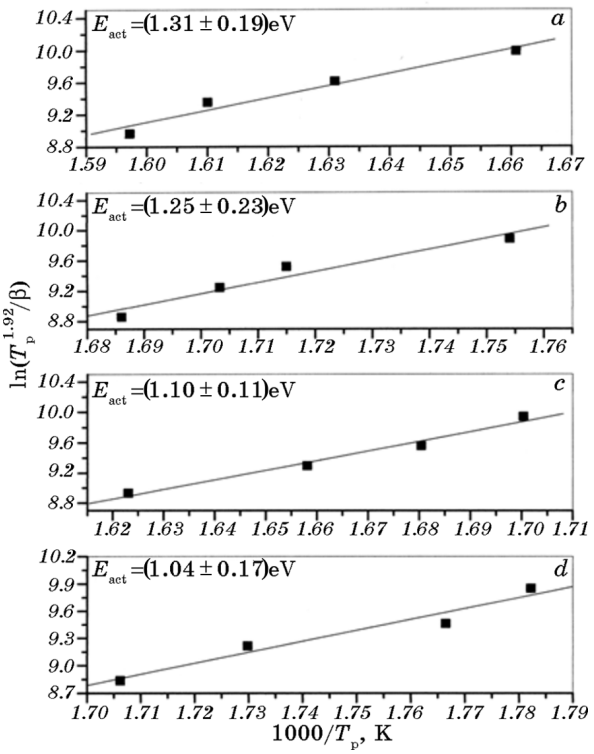

Fig. 7. Starink's plot to obtain the activation energy values of the $D0_3$ ordering process in: Fe–25Al–25Cr (*a*), Fe–25Al–9Cr (*b*), Fe–28Al–4Cr (*c*), Fe–27Al–2Cr (*d*) alloys.

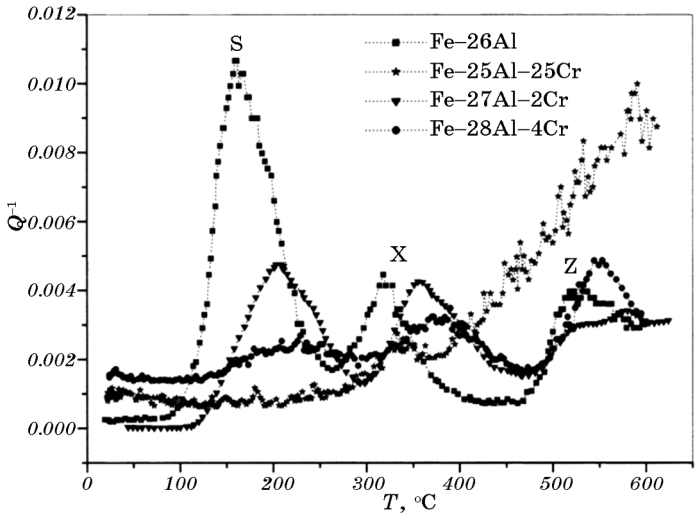

Fig. 8. $Q^{-1}(T)$ in homogenised and water quenched Fe–26Al and Fe–25Al–Cr alloys for 1–2 Hz.

the heights of S and X peaks is observed with the increase of Cr amount, until their disappearance with addition of 25 at.% Cr.

The decrease in the Snoek-type and X peaks heights is probably caused by the trapping of carbon atoms in chromium carbides, while a shift of the Snoek-type peak to higher temperature is the result of the C–Cr interaction in solid solution. The Snoek-type and X peaks can hardly be distinguished in some cases: only by stepwise Cr adding into Fe–Al.

The Zener relaxation peak—reorientation of pairs of substitute atoms under applied periodic stress—is slightly broadened and shifted to higher temperatures as compared to binary Fe–Al alloys. The Al–Cr and Cr–Cr interactions imply a broadened Zener peak at higher temperature as compared to binary Fe–26Al, because the effects of Al and Cr pairs are superposed (Fig. 8). No clear peaks were recorded in Fe–25Al–25Cr alloys at the position that corresponds to the Zener peak in the binary Fe–25Al composition; may be the Zener peak will appear around or above 600°C, while the Snoek-type peak disappears in this alloy because of high Cr amount.

3.6. Effect of Chromium on the Microhardness of Studied Alloys

Several theoretical and experimental works show that the mechanical properties of Fe–Al alloys can be improved by the addition of chromium. According to the obtained results of the microhardness measurements for all studied alloys homogenised 1 h at 1000°C, water quenched and then annealed at 300°C (temperature of formation of $D0_3$

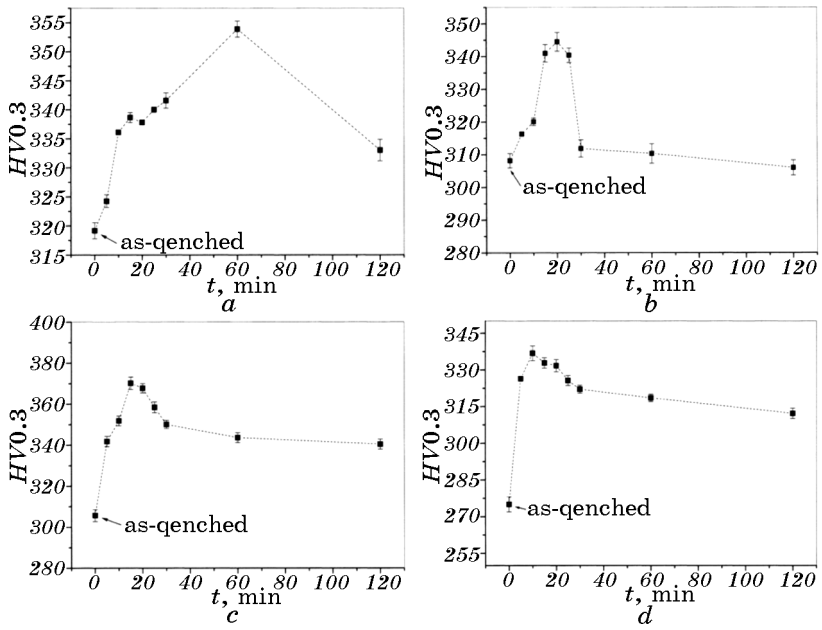

Fig. 9. Variation of the microhardness as a function of annealing time at 300°C for: Fe–25Al–25Cr (*a*), Fe–25Al–9Cr (*b*), Fe–28Al–4Cr (*c*), Fe–27Al–2Cr (*d*) alloys.

ordered phase) for various times, the formation of this phase leads to the increase in the microhardness (Figs. 9, *a*–*d*).

The increase in microhardness with the increase in annealing time takes place until a certain point: 60 min for Fe–25Al–25Cr alloy, 20 min for Fe–25Al–9Cr alloy, 15 min for Fe–28Al–4Cr alloy and 10 min for Fe–27Al–2Cr alloy; then hardness decreases. Increase in hardness can be explained by the increase in order degree and, consequently, by increase in the volume fraction of the $D0_3$ antiphase domain until the complete transformation of the α disordered phase to the $D0_3$ ordered phase.

Beauchamp *et al.* (Ref. 2 cited by [30]) show that annealing at temperatures close to the critical temperature (formation of the $D0_3$ ordered phase) reduced the energy of the antiphase boundaries with their separation by approximately two, three or five atomic plains. The reduction in the energy of these boundaries implies an increase in mobility of dislocations and leads to a better ductility (Ref. 1–5 cited by [17]). The decrease in the microhardness is caused by the coalescence of some antiphase boundaries [18]. The comparison between the microhardness values of studied alloys shows that the maximum value is reached faster in the alloy with slight Cr addition; this difference can be explained by the effect of the chromium addition that slows the process of coales-

cence of the antiphase boundaries [18].

4. SUMMARY

The advanced properties of the Fe–Al alloys create a wide prospect for their industrial applications. However, these materials present a poor ductility at ambient temperature, which can be improved by the addition of the third element. Chromium is the favourable element for this improvement. In this paper, we studied the effect of this element on the order–disorder transitions in different ternary Fe–Al–Cr alloys.

Dilatometric and DSC studies show the different transitions existing in different studied Fe–Al–Cr alloys, and show that the addition of Cr in Fe_3Al compound slows the $D0_3$ ordering. This is additionally confirmed by the obtained values of activation energy of the ordering process of the $D0_3$ ordered phase formed in studied alloys. Starink's method permits to estimate the value of this energy in different studies alloys, and shows that the ordering process of $D0_3$ ordered phase requires more energy in Fe_3Al–Cr alloys with higher Cr amount (see Table 3). XRD and TEM studies show that water quenching from high temperature cannot suppress the formation of $B2$ ordered particles in overstoichiometric Fe_3Al alloys.

Annealing at temperature close to the temperature of $D0_3$ ordered phase formation leads to an increase of the microhardness, which can be explained by the increase of the fraction of the $D0_3$ antiphase domain boundaries until the complete formation of $D0_3$ ordered phase. The maximum value of this microhardness is reached faster with lower Cr addition than in the alloy with high percentage of Cr; thus, Cr addition slows the process of coalescence of antiphase boundaries.

Chromium has also an effect on the anelastic relaxation in these alloys; it leads to the decrease of the heights of the Snoek-type peak and the peak at higher temperature that is tentatively explained by vacancies and carbon complexes. The Snoek- and Zener-type peaks shift to higher temperatures with increase in Cr content in alloys. A broadening of the Zener peak in presence of Cr can be explained by contribution to Zener relaxation not only by Al–Al, but also by Cr–Cr and Al–Cr atom pairs.

REFERENCES

1. G. Niewielski, D. Kuc, I. Schindler, and I. Bednarczyk, *Archives of Materials Science and Engineering*, **29**: 117 (2008).
2. G. Sauthoff, *Intermetallics* (New York: VCH Weinheim: 1995).
3. Z. Li and W. Gao, *Intermetallics Research Progress* (Ed. Y. N. Berdovsky) (New York: Nova Science Publisher Inc.: 2008).
4. V. A. Udovenko, S. I. Tishaev, and I. B. Chudakov, *Doklady Physics*, **38**: 168

(1993); idem, *Russian Metallurgy (Metally)* **1**: 98 (1994); idem, *Solid State Phenomena*, **137**: 109 (2008).
5. M. Ishimoto, H. Numakura, and M. Wuttig, *Mater. Sci. Eng. A*, **442**: 195 (2006).
6. I. S. Golovin, Z. Belamri, and D. Hamana, *J. Alloys Compd.*, **509**: 8165 (2011).
7. A. M. Russell, *Intermetallics Research Progress* (Ed. Y. N. Berdovsky) (New York: Nova Science Publisher Inc.: 2008); A. M. Russel, *Advanced Eng. Materials*, **5**, No. 9: 629 (2003).
8. M. H. G. Jacobs and R. Schmid-Fetzer, *CALPHAD: Computer Coupling of Phase Diagrams and Thermochemistry*, **33**: 170 (2009).
9. S. Zuquing, Y. Wangyue, S. Lizhen, H. Yuanding, Z. Baisheng, and Y. Jilian, *Mater. Sci. Eng. A*, **258**: 69 (1998).
10. I. S. Golovin, S. V. Divinski, J. Čížek, I. Procházka, and F. Stein, *Acta Mater.*, **53**: 2581 (2005).
11. I. S. Golovin, *Mater. Sci. Eng. A*, **442**: 92 (2006).
12. V. K. Sikka, S. Viswanathan, and C. G. McKamey, *Structural Intermetallics* (Eds. R. Darolia, J. J. Lewandowski, C. T. Liu, P. L. Martin, D. B. Miracle, and M. V. Nathal) (TMS: 1993), p. 483.
13. C. G. McKamey, J. A. Horton, and C. T. Liu, *J. Mater. Res.*, **4**: 1156 (1989).
14. D. G. Morris, M. Dadras, and M. A. Morris, *Journal de Physique. Colloque C7*, **111**, No. 3: 429 (1993).
15. G. Sharma, K. B. Gaonkar, and P. R. Singh, *Mater. Lett.*, **61**: 971 (2007).
16. D. Hamana, L. Amiour, and M. Bouchear, *Mater. Chem. Phys.*, **112**: 816 (2008).
17. I. S. Golovin, A. Strahl, and H. Neuhauser, *Int. J. Mater. Res.*, **42**: 1078 (2006).
18. M. Boufenghour, A. Hayoune, and D. Hamana, *J. Mater. Sci.*, **39**: 1207 (2004).
19. O. A. Lambri, J. I. Pérez-Landazábal, V. Recarte et al. (to be submitted to *Intermetallics*).
20. M. J. Starink, *Thermochim. Acta*, **404**: 163 (2003).
21. H. E. Kissinger, *Anal. Chem.*, **29**: 1702 (1957).
22. T. Ozawa, *J. Therm. Anal.*, **2**: 301 (1970).
23. J. Benard, A. Michel, J. Philibert, and J. Talbot, *Métallurgie Générale. 2eme édition* (Paris: Masson: 1984).
24. M. S. Blanter, I. S. Golovin, H. Neuhäuser, and H.-R. Sinning, *Internal Friction in Metallic Materials: Handbook* (Berlin–Heidelberg: Springer: 2007).
25. I. S. Golovin, M. S. Blanter, and R. Schaller, *phys. status solidi (a)*, **160**: 49 (1997).
26. I. S. Golovin, *J. Alloys Compd.*, **310**: 356 (2000).
27. K. Tanaka and K. Sahashi, *Trans. JIM*, **3**: 130 (1971).
28. I. S. Golovin, S. B. Golovina, A. Strahl, H. Neuhäuser, T. S. Pavlova, S. A. Golovin, and R. Schaller, *Scr. Mater.*, **50**, No. 8: 1187 (2004).
29. M. S. Blanter, I. S. Golovin, and H. R. Sinning, *Scr. Mater.*, **52**, No. 1: 57 (2005).
30. D. G. Morris and M. Leboeuf, *Philos. Mag. Lett.*, **70**: 29 (1994).